Available online at www.sciencedirect.com
SCIENCE DIRECT
Journal of Chromatography B, 826 (2005) 8–16
JOURNAL OF CHROMATOGRAPHY B
www.elsevier.com/locate/chromb

# Fast "hyperlayer" separation development in sedimentation field flow fractionation☆

James R. Kassab[a,b], Philippe J.P. Cardot[a,*], Richard A. Zahoransky[b], Serge Battu[a]

[a] *Laboratoire de Chimie Analytique et de Bromatologie, Université de Limoges, Faculté de Pharmacie, 2 Rue du Dr. Marcland, F-87025 Limoges, Cedex, France*
[b] *International Quality Network, Nanoparticles and Bioparticles Project, University of Applied Sciences, Badstr. 24, D-77652 Offenburg, Germany*

Received 19 May 2004; accepted 9 June 2005
Available online 11 July 2005

**Abstract**

Specific prototypes of sedimentation field flow fractionation devices (SdFFF) have been developed with relative success for cell sorting. However, no data are available to compare these apparatus with commercial ones. In order to compare with other devices mainly used for non-biological species, biocompatible systems were used for standard particle (latex: 3–10 μm of different size dispersities) separation development. In order to enhance size dependent separations, channels of reduced thickness were used (80 and 100 μm) and channel/carrier-phase equilibration procedures were necessary. For sample injection, the use of inlet tubing linked to the FFF accumulation wall, common for cell sorting, can be extended to latex species when they are eluted in the Steric Hyperlayer elution mode. It avoids any primary relaxation steps (stop flow injection procedure) simplifying series of elution processing. Mixtures composed of four different monodispersed latex beads can be eluted in 6 min with 100 μm channel thickness.


*Keywords:* Sedimentation field flow fractionation; Latex particles; Steric Hyperlayer

## 1. Introduction

The field flow fractionation separation concept was proposed by Giddings in the 1960s [1]. It was theoretically described as one of the most versatile separation concepts in particular in the macromolecule to colloidal domain [2,3]. However, despite its versatility and separation capacities, it was not associated with the economic success of chromatography or electrophoresis. This is the case of sedimentation FFF, which gained renown in cell sorting [4–8]. The most simple sedimentation FFF device uses simple earth gravitational field (GFFF), it is easy to build and offers an original potential for applications in cell sorting [4–6]. During the last decade, series of biocompatible laboratory-designed multi gravitational devices (SdFFF) opening new and unmatched cell separation opportunities [7,8], were set up. The objective of this report is to provide instrumental and methodological comparison data of these SdFFF devices designed for cell sorting with commercialized ones. In order to establish the basic characteristics of separation comparison, elutions were performed with certified particles used as standards.

Field flow fractionation [9], follows a constant but relatively confidential development, and is now well described [4–6,10–15].

The devices used in this report have some specific characteristics, which are:

- the sample is introduced in the FFF separation system by means of a chromatographic injection loop when both the flow and external field are established;

☆ Parts of this work, of critical interest in cell sorting with Field Flow Fractionation were described during: 9th SNCN Symposium Bordeaux, France, May 5–7, 2004.

* Corresponding author. Tel.: +33 5 55435857; fax: +33 5 55435859.
*E-mail address:* cardot@unilim.fr (P.J.P. Cardot).

1570-0232/$ – see front matter © 2005 Elsevier B.V. All rights reserved.
doi:10.1016/j.jchromb.2005.06.020

- the FFF channel inlet tube is connected to the accumulation wall of the channel. The sample injection procedure avoids therefore any "primary relaxation step" also described as "stop flow injection"[16,19];
- channels of reduced thickness are used to enhance the effect of the lifting forces [16–19], channels walls are made of polystyrene.

In sedimentation field flow fractionation (GFFF, SdFFF) the elution model for the micron particles is generally described as "Steric Hyperlayer" [9,16–19]. Models of the Hyperlayer focusing of particles in the micrometer range (diameter) eluted in FFF have been published [9,16,18,19]. It is a phenomenon driving to an equilibrium position in the channel thickness and can be considered accurate assuming that:

- in identical experimental conditions (channel, carrier phase composition flow rate, temperature), the kinematics of particles of same size, shape, and density toward equilibrium are analogous;
- flow injection reduces particle/wall interactions to acceptable recovery (over 70%);
- the reversible (or not) trapping of sample particles in the channel is not size selective (the particle size distribution of the sample eluted is identical to the particle size distribution of the sample injected);
- limited particle/wall retardation effects occur.

In such configurations, spherical particles of different sizes are eluted according to their size, the larger ones being eluted first, while those of identical size can be separated according to their density [20,21], the more dense being eluted later. In the case of the different standards latex species assayed in that report, it is assumed that their volumic mass are rather identical, leading to the consequence that the separations shown were essentially size dependent.

## 2. Experimental

### 2.1. Sedimentation field flow fractionation systems

Two different sedimentation FFF devices were used in this study. They consist of an FFF separator connected to a UV–vis detector and to a classical HPLC pump via a sample chromatographic-like device [15,22,23]. In both cases, FFF channels consist of two polystyrene plates, one described as the depletion wall and the other called accumulation one, separated by a Mylar® band in which the channel is manually cut. The thickness of the Mylar® defines the channel's height. Two ribbon like channels where therefore set up, channel I whose dimensions were 784 mm × 15.5 mm × 0.08 mm (length, breadth, thickness) and channel II 781 mm × 15 mm × 0.100 mm. Both channels were designed with two V-shaped ends (70 mm); giving respective theoretical channel volumes of 960 and 1066.5 μL. These assemblies were sealed into centrifuge baskets (rotor bowls) of analogous diameter, being careful to avoid deforming the channel's parallelepiped shape during the sealing. These channels were connected to the other devices by means of laboratory designed rotating seals and commercial connecting tubes. The rotating seals were made of two symmetrical planar disks of different composition (metal to polymer) drilled to connect the tubes in their center. The sample inlet tubes for channel I (i.d. = 0.256 mm, 0.514 μL/cm) and for channel II (i.d. = 0.384 mm, 1.140 μL/cm) were connected to their relative channel via the accumulation wall. The tube and rotating seal volume were experimentally measured and found to be 35 and 79.4 μL for channels I and II, respectively. The void volumes of the channel outlet tubes (same i.d. as the inlet tubes) and rotating seals were, respectively, 33.5 and 76.3 μL. The respective total FFF system void volumes are, respectively, 1040 ± 20 μL ($n$ = 20) for channel I and 1272 ± 16 μL ($n$ = 15) for channel II. Void volumes were measured using acetone (1%, v/v) elutions in the carrier phase. Sedimentation fields are expressed in rpm (rpm: rotation per minute) which can be transformed into units of gravity (1 g = 980 cm/s$^2$) by means of both the measured rotational speed (rpm) and the channel radius, $r$ (cm) according to the following equation:

$$G = \left(\frac{\text{rpm} \times 2\pi}{60}\right)^2 \times r \quad (1)$$

The channel radii measured after sealing were 13.5 and 14.1 cm for channels I and II, respectively. Knauer HPLC pumps Type 364 (Knauer, Berlin, Germany) were used to produce the carrier flow. In each experiment, the flow rates were systematically measured, and experimental values were used for data interpretation. Samples were injected using a Rheodyne model 7525 loop injector (Rheodyne. Inc., Cotati, CA). The injection volumes were either 12 or 20 μL. The carrier and sample dilution medium, were doubly distilled deionized water containing different percentages (w/v) of appropriate surfactants. The first one FL70 was provided by Fisher Scientific (Fisher Scientific, Elancourt, France), and is of historical significance. FL70 is a surfactant of complex composition commonly used in the early development of FFF. It was often employed for latex beads separations, however that surfactant is no longer available. The second surfactant was simple sodium dodecyl sulfate (SDS, Sigma–Aldrich, Lyon, France) which was particularly interesting in association with polystyrene channel walls. Particle elution was monitored using Knauer UV–vis photometers 731 (Knauer, Berlin, Germany) operating at 254 nm. Signals were systematically recorded by means of a 14 bytes analogue-to-digital converter which has been already described [24]. The signal acquisition rate was set to 2 Hz.

Table 1
Polystyrene standard characteristics given by the manufacturer (Duke Scientifics)

| Standard | Certified mean diameters (μm) ± 2σ | CV (%) |
|---|---|---|
| 1 | 3.063 ± 0.027 | 43.0 |
| 2 | 4.988 ± 0.035 | 1.0 |
| 3 | 6.992 ± 0.050 | 1.0 |
| 4 | 9.975 ± 0.061 | 14.7 |

Data correspond to the particle lot used for experiments. Values were measured by the manufacturer using Nist (National Institute of Standards and Technology) compliant procedures. In the case of Microsphere® Size Standards, the size determination method was microscopy. Mean and CV% were determined from number measurements.

### 2.2. Samples, elution procedures and peak profile analysis

All polystyrene latex standards used in this work were obtained from Duke Scientific corporation (Palo Alto, CA). Their mean diameters and coefficient of variation (CV%) are shown in Table 1. The spheres are purported to have an average density of 1.05 g/cm$^3$ and can be considered as monodispersed in size if associated with low CV% values and polydispersed if CV% are higher than 10%. For test separations in the FFF system, the standards were diluted ~100–200 times with the carrier phase and supplemented with acetone (0.1%, v/v) for void volume qualification. All elutions were performed in the "flow mode", i.e. the sample was introduced in the FFF system once field and flow were established. Therefore, the separation process was almost analogous to those performed in cell sorting, simplifying considerably the operating conditions. All peak profile characteristics were analyzed using peak statistical moment calculations.

## 3. Results and discussion

### 3.1. Channel design and conditioning

Once the channel dimensions are properly cut from a Mylar sheet whose thickness defines the channel height, it is sealed in the centrifuge basket by means of two soft polystyrene plates. The relative flexibility of such systems may produce channel geometry deformations which must be controlled. If a sealing is properly performed, the acetone elution profile must show two characteristics: its elution volume must correspond to the geometrical channel void volume (5% error tolerated) and the peak profile must be monomodal (chromatographic like) as shown for the first peak of the fractogram plotted in Fig. 1. If discrepancies appear in terms of volume or peak shape, the sealing must be redone.

In order to comply as closely as possible with literature data on latex beads in sedimentation field flow fractionation [11,25], the historically used FL70 surfactant was used. However, a surprising result with polystyrene walls shown in Fig. 1 was observed. Latex (diameter: 5 μm) suspension elutions

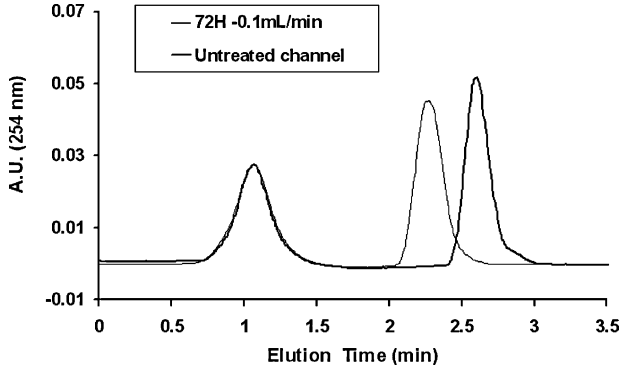


Fig. 1. Effect of channel treatment on elution profile. Latex beads, 5 μm in diameter 1% CV. Mobile phase composition: FL70/water 0.1% (w/v). Rotation speed: 436.5 rpm. Measured flow rate: 0.96 mL/min. Flow and field established injection procedure of 12 μL 0.02% latex suspension in mobile phase. Photometric detection (254 nm). Channel/mobile phase equilibration procedure: channel is flowed with mobile phase at low flow rate for 72 h.

were performed directly after proper sealing and fractograms were obtained (Fig. 1 untreated channel). In order to test the accuracy of the sealing and detect whether short term deformations could be obtained after channel use, the FFF system was kept in rotation and the carrier phase flowed through at 0.1 ml/min for 72 h. An elution control was then performed. It showed a shift in retention (Fig. 1: treated channel). Latex species were less retained when carrier phase was pumped for a long period. The void volume mode and profile characteristics of both fractograms were very similar indicating that the shift was not caused by mechanical deformations after three days. Long term elution controls (10 days, not shown) led to fractograms analogous to the ones obtained after 72 h of continuous carrier flow. Such results can be interpreted by the possible set up of surfactant/channel wall interactions. Obviously polystyrene walls must be conditioned by the carrier before any elution measurements. If different carriers are to be used in the same channel, long term reconditioning and washing procedures must be used for example, switching from FL70 to SDS, requires:

(a) flushing out FL70 surfactant using distilled water;
(b) 72 h of SDS/distilled water (0.1%, w/v) flowing in the channel.

Once the channel is properly conditioned geometrically as well as chemically, it is ready for further investigations.

### 3.2. Elution characteristics

Channel I is associated with one of the smallest void volume ever used in SdFFF. It is therefore necessary to explore and qualify the elution and separation properties of such new system.

#### 3.2.1. Reproducibility

The possibility to use established flow injections considerably simplifies the elution procedure; the flow rate is

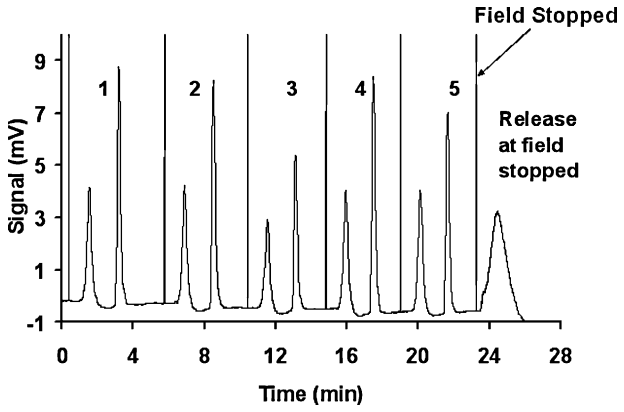


Fig. 2. Elution reproducibility. Latex beads, 7 μm in diameter 1% CV. Mobile phase composition FL70/water 0.1% (w/v) average rotation speed 437 ± 1.5 rpm ($\sigma$, $n = 8$). Average flow rate:1.0 ± 0.2 mL/min ($\sigma$, $n = 6$). 0–10 mV signal corresponds to 0–0.06 A.U.@254 nm.. Flow and field established injection procedure of 12 μL 0.02% latex suspension in mobile phase. Fractogram elution characteristics described in Table 2.

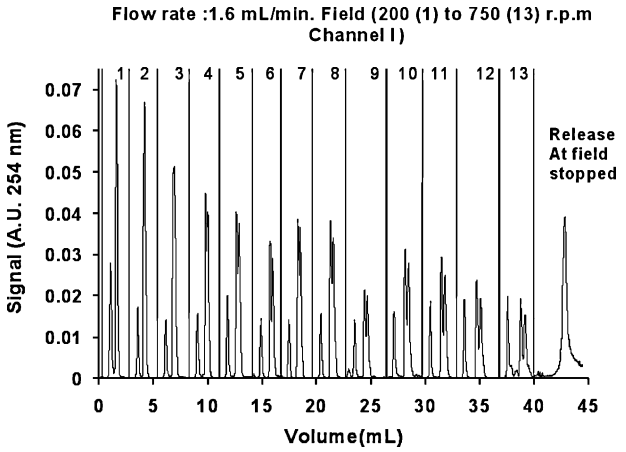


Fig. 3. Field dependent separation sequence of 5 and 7 μm latex particles. Channel I: carrier phase 0.1% (w/v) SdS/water, injection of 20 μL 0.02% latex mixture suspension in established flow. Flow rate: 1.6 mL/min. External field produced by basket rotation ranging from 200 to 750 rpm (runs 1–13 correspond, respectively from 200, 248, 310, 352, 403, 445, 508, 552, 571, 604, 634, 706, 756 rpm).

definitively established and monitored, as well as the rotation speed generating the field strength. Short term reproducibility is therefore possible as shown in Fig. 2. Each fractogram, consists of two peaks, the first eluted one represents the elution of acetone, and the second, the elution of latex particles (7 μm). Remarkable elution reproducibility is observed in terms of retention and peak profile characteristics as shown in Table 2. However, the peak intensities of the void volume and latex peaks appears relatively different from one elution to another. One must have in mind that the sample is a suspension and so far it is relatively difficult to inject perfectly reproducible particle quantities in the SdFFF system via manual injection loop. With channel I each elution was performed in less than 4 min. Seven micrometer latex beads were eluted with a retention ratio value of 0.5. After five consecutive elutions, the field was stopped and as a consequence, a peak was observed, whose fraction collection shows the presence of latex beads, a sample release at field stopped is therefore observed.

### *3.2.2. Possible flow injections leading to rapid separation development*

In order to test the separation potentials of channel I, a mixture of 5 and 7 μm monodispersed latex beads was prepared in the carrier containing 0.1% (w/v) SDS. Practically, the easiest elution parameter to monitor is field strength (rotation speed).

Separation development scheme appears to be analogous to that encountered in HPLC. The first, objective is retention. For that purpose relatively high flow rates will be used, in order to reduce elution time, and to create strong shear forces at the channel accumulation wall, thereby enhancing recovery. Retention is, therefore, mainly determined by the intensity of the external field generated by rotation speed as shown in Fig. 3. Then in a second step, once appropriate retention has been obtained, flow rate is decreased to enhance selectivity as shown in Fig. 4. Flow rate is first set at 1.6 mL/min which is a good compromise between flow pressure in the rotating seals, reduced elution time and photometric detector stability. Between every injection the field is increased gradually. A sequence of 13 elutions was performed with an increasing field ranging from 200 to 750 rpm as shown in Fig. 3. For every run, elution time was less than 3 min. For the three first injections, no separation was observed while for the thirteenth one, the latex beads were completely separated. However, if high fields (700 rpm)

Table 2
Reproducibility data from Fig. 2 sequence

| Experiment | Acetone elution time (min) | $N^*$ acetone | Latex 7 μm elution time (min) | $N^*$ latex | Latex peak intensity (mV) |
|---|---|---|---|---|---|
| 1 | 1.16 | 85 | 2.82 | 1253 | 9 |
| 2 | 1.14 | 77 | 2.76 | 1215 | 8.64 |
| 3 | 1.14 | 90 | 2.72 | 1000 | 6 |
| 4 | 1.13 | 88 | 2.68 | 950 | 9 |
| 5 | 1.10 | 90 | 2.63 | 900 | 7.56 |
| Average | 1.13 | 86 | 2.72 | 1063 | 8.04 |
| Standard deviation | 0.025 | 5.4 | 0.075 | 160 | 1.3 |

$N^*$: plate number. Peak variance and elution time were calculated using the statistical moment method, elution time (=first moment), variance (=second centered moment).

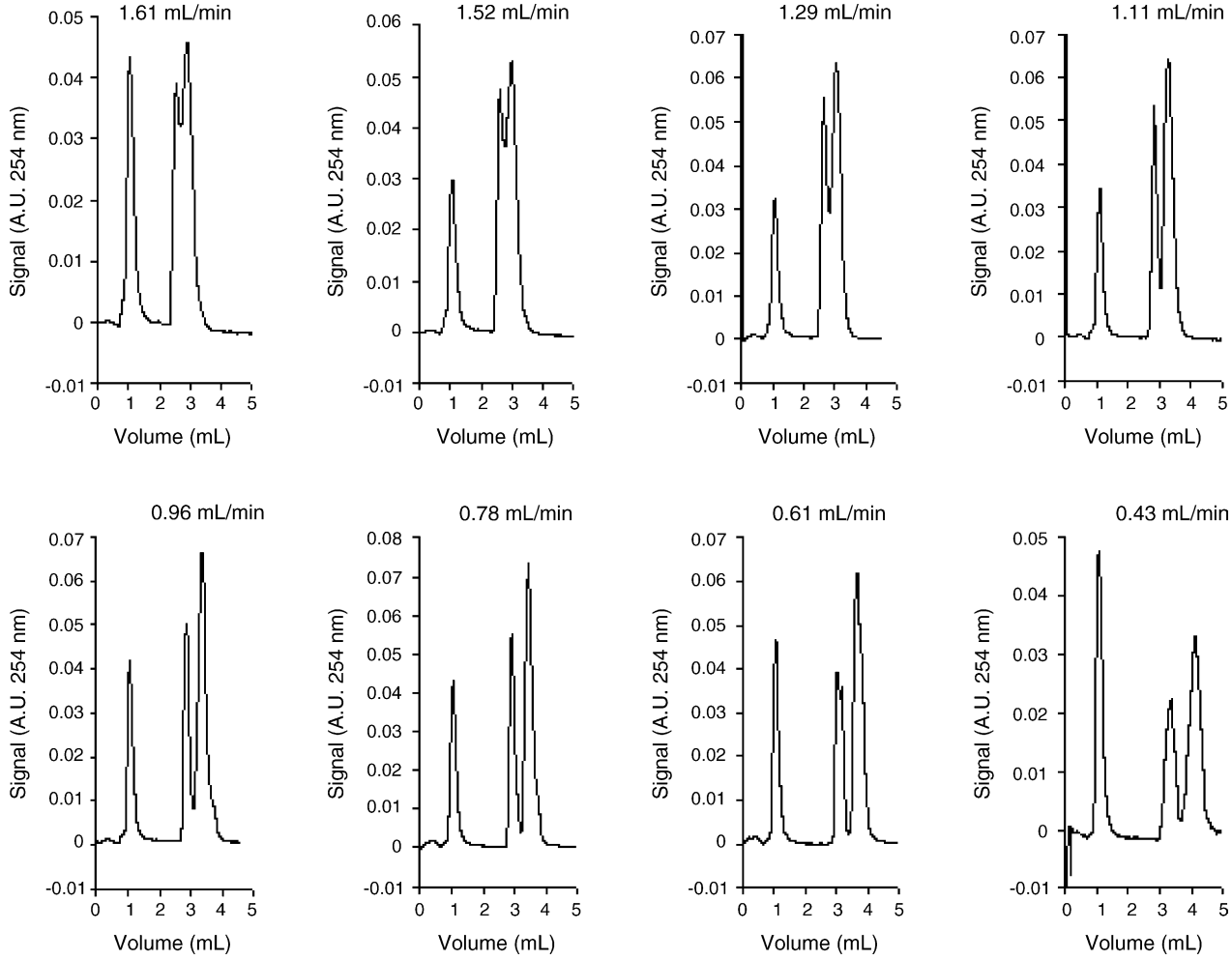


Fig. 4. Flow rate dependent separation optimization sequence of 5 and 7 μm latex particles. Channel I: External field produced by rotation speed of 550 rpm. All other conditions described in Fig. 3. Carrier phase 0.1% (w/v) SdS/water, flow injection 20 μL 0.02% latex mixture suspension in established flow.

were applied, distorted latex bead peak profiles (35–40 mL in Fig. 3) were observed. Resolution is increased with increased field. A 0.54 resolution value was found at run 4 (352 rpm), and increased to 0.83 at run 12 (706 rpm). This effect can be interpreted in the context of the "Hyperlayer" elution mode. At a given flow rate, high external fields drive the latex species very close or even "on" the accumulation channel wall, leading to complex wall/particle interactions. These interactions may be at the origin of the sample trapping. Therefore, preliminary guidelines are given for separation development in channel I. They indicate the use of fields less than 700 rpm for flow rates less than 1.6 mL/min. In order to optimize separation, an intermediate field (550 rpm) was chosen. In that condition, latex beads are completely resolved from the void volume peak and resolution initiated. In order to optimize resolution, we can consider the hypothesis that both latex populations will undergo different lifting force intensities (they have been described as being strongly size dependent [17–19]). Flow rate dependent elutions at a constant external field were consequently performed. This step is analogous to the one encountered in HPLC for molecule separations, where, when the solvent strength is defined, mobile phase composition is modified to enhance selectivity. Elution sequences could not be done in these cases as they required a detector equilibration time. Fractogram series are shown in Fig. 4. From slightly separated profiles obtained at 1.6 mL/min, almost complete separation was obtained using flow rates ranging from 0.96 down to 0.43 mL/min. The optimum resolution was calculated at 0.83 mL/min, as shown in Table 3. The fractogram series in Figs. 3 and 4, behave similarly. When at given flow rates, fields were too intense (higher than 700 rpm: as seen on Fig. 3) or when for a given field, flow rates were very low (lower than 0.7 mL/min as seen on Fig. 4) resolution was degraded. This was due to the distortion of every latex peak profile. Such results have to be interpreted in light of the Steric Hyperlayer elution model [16–19] where for a given particle the external field versus flow balance focalizes a given specie (i.e. latex bead) in given stream line within the channel thickness. If too intense fields or too low flow rates are used, the elution mode tends to be "Steric" with complex particle/wall interactions whose consequences are peak distortions and reduced recovery. At

Table 3
Flow rate (mL/min) dependent resolution optimization of 5 and 7 μm latex beads

| Flow rate | Resolution |
|---|---|
| 1.61 | 0.53 |
| 1.52 | 0.48 |
| 1.29 | 0.57 |
| 1.11 | 0.62 |
| 0.96 | 0.70 |
| 0.78 | 0.83 |
| 0.61 | 0.59[a] |
| 0.43 | 0.70[a] |

Peak retention and variance characteristics measured using the statistical moment method. Peak width = 4$\sigma$.
[a] Peak profile distortion.

a given flow rate, too intense fields surpass the lifting forces, driving the particle very close to the accumulation wall. Analogously, for a given field, reduced flow rates diminished lifting force intensities also driving the species very close to the accumulation wall.

At the end of the sequences in Figs. 3 and 4, a signal release (not shown for Fig. 4) was obtained. This was due to the remaining trapped particles in the channel when the field was stopped. This release is analogous to that in Fig. 2. The SDS surfactant, used in combination with polystyrene channel walls cannot eliminate some sample trapping already observed with FL70 in Fig. 2.

#### 3.2.3. Particle trapping

When the fraction corresponding to the peak release obtained when the field is stopped (40–50 min of Fig. 3), was collected and analyzed, particles were observed. This, points out a major complication in FFF. The introduced sample was not completely eluted. The absence of sample balance conservation (what is eluted is what is injected) limits FFF to separation trends at present and complicates any quantitative analysis. It is necessary to better understand the complex interactions of latex particles in a given carrier phase versus channel wall characteristics. Irreversible as well as reversible particle trapping may be discussed in the future using guidelines given by van Oss in terms of sorption energies [26,27]. In our experience it appears that elution recovery can vary from 40% to 95% depending on FFF operating conditions and the type of sample used. In Figs. 2 and 3, it appears that methodological precautions must be taken when latex elutions are performed, in terms of channel reconditioning. Short term channel washing, can be performed by simply flowing the carrier phase at 0.5 G field (0 rpm). This operation should be performed every working day (every 30–50 runs or as soon as results are not reproducible. Particle washing after every run is not associated with a "signal" detection when the field is stopped. Long term channel reconditioning can be time consuming, using water for latex bead elution or special cleaning agents in the case of biological materials containing lipids and proteins like cells. The washing procedure should be followed by 72 h channel reconditioning with the carrier phase.

Table 4
Latex resolution and size selectivity in channel II

| Resolution | A | B | C | D |
|---|---|---|---|---|
| 10–7 μm | 0.60 | 0.52 | 0.53 | 0.58 |
| 7–5 μm | 0.66 | 0.53 | 0.60 | 0.70 |
| 5–3 μm | 0.50 | 0.43 | 0.34 | 0.49 |
| Cumulative resolution | 1.76 | 1.48 | 1.47 | 1.78 |
| Size selectivity characteristics: log(tr) = slope × log(size) + intercept | | | | |
| Slope | −0.66 | −0.57 | −0.57 | −0.53 |
| Intercept | 0.94 | 0.93 | 0.97 | 0.96 |

Peak retention and variance characteristics measured using the statistical moment method.

### 3.3. Thicker channel resolution

We demonstrated that size selective separations can be obtained in few minutes with a reduced void volume. Consequently a reduced dilution factor enhancing signal sensitivity was obtained. Unfortunately very few data on equivalent channels are available. If channel I appeared to be very effective for the separation of species very close in size, such as 5 and 7 μm latex beads or smaller ones, larger ones (10 μm or more) were not retained properly.

In order to provide comparative data with those available in the literature [28–31] and to increase the peak capacity, a lightly thicker channel was used (channel II). Fractograms obtained under different elution (field and flow) conditions are shown in Fig. 5. A protocol analogous to the one used for channel I was used and two different flow rates were used (1.8 mL/min for Fig. 5A and B and 1 mL/min for Fig. 5C and D) as well as two external fields (650 rpm for Fig. 5A and C and and 829 for Fig. 5B and D). All separations showed similar summarized resolutions while the different flow and field couples enhanced different adjacent peaks resolutions as shown in Table 4. In every case the best resolution was obtained for both monodispersed populations (7 and 5 μm). Large optimization sequences were therefore possible in order to complete these separations. Table 4 shows that condition D (1 mL/min, 829 rpm) was associated with the best cumulative and particle to particle resolutions. Nevertheless, the best 7–5 μm resolution was found using channel I (Table 3). Considering the different size distributions of the latex particles involved in the separations shown in Fig. 5, it is obvious that baseline peak resolutions could not be obtained. Some particles (10 and 3 μm) were associated with broad size distribution. In the case of 3 μm latex beads a 43% CV indicates that particle size ranged from almost 2 to 5 μm. The 3 μm latex population contains particles in the 5 μm range (average ± 2$\sigma$). An analogous situation is found for 10 μm (14.7% CV) latex beads, indicating a continuous size distribution from 10 μm down to 7 μm. The consequences are that baseline resolution of 10 and 7 μm latex beads as well as of 5 and 3 μm ones are intrinsically impossible. Experimental condition D therefore seems to be optimized. In these conditions, and in contrast to channel I, 7 and 5 μm populations have a resolution less than 0.8.

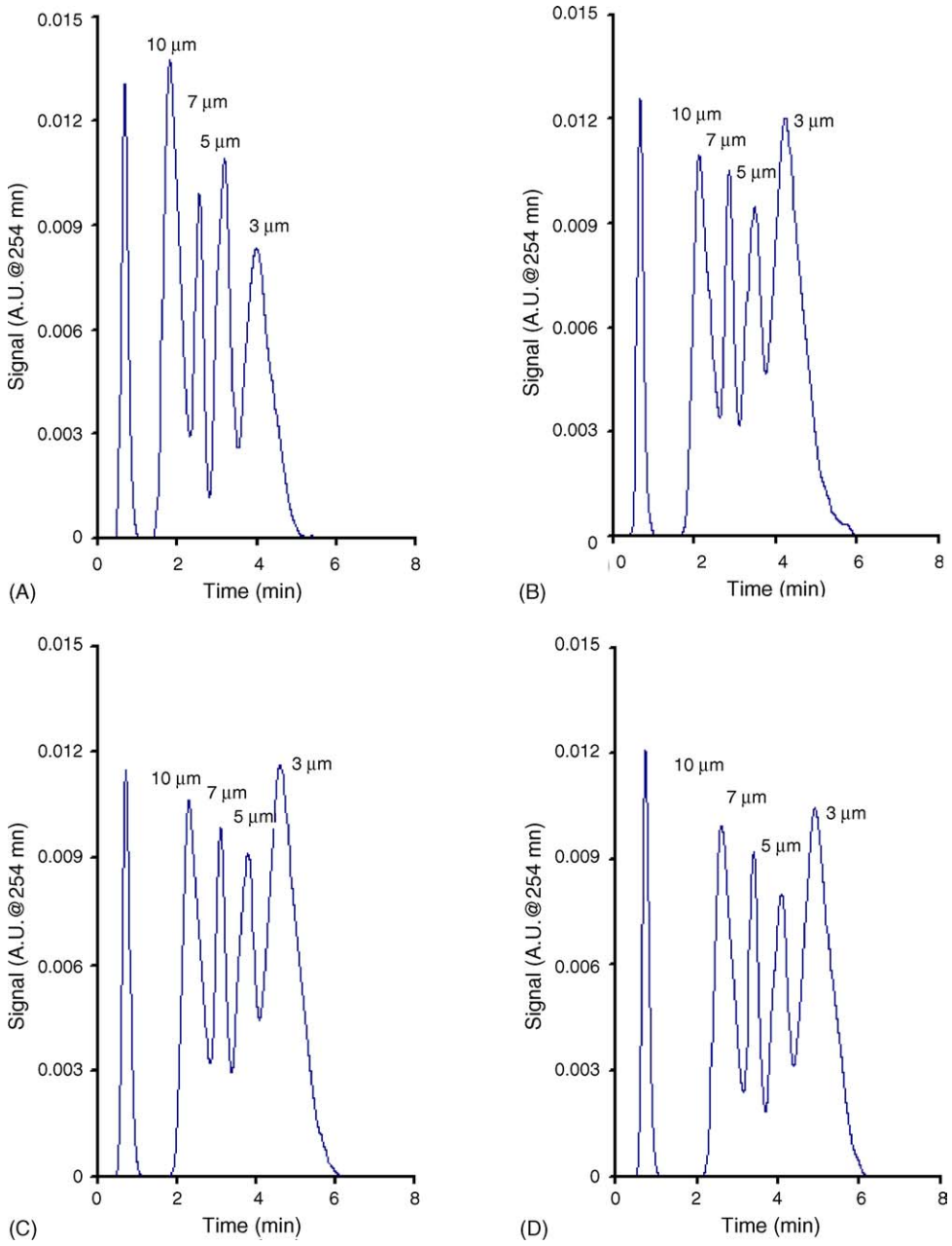


Fig. 5. Latex mixture fractograms. Optimized separations of latex particles of different size and polydispersity in channel II, carrier phase 0.1% (w/v) SdS/water, flow injection: 20 μL 0.02% latex mixture suspension in established flow. Flow and field experimental conditions: (A) 1.8 mL/min 650 rpm; (B) 1.8 mL/min 829 rpm; (C) 1 mL/min 650 rpm; (D) 1 mL/829 rpm.

However, the interest in the elution of a four particle population (10, 7, 5 and 3 μm) is to draw size based selectivity curves for each established field/flow condition as shown in Fig. 6A. In any experimental conditions (A–D) linear curves were found. Curve characteristics (regression parameters shown in Table 4) demonstrated a size based elution order whose characteristics depended on the experimental conditions (field and flow). Such linear size selectivity curves for latex beads have already been demonstrated in the literature dealing with such separations, but Fig. 6A is one of the first demonstrations using the experimental conditions presented here, i.e. avoiding any stop flow injection procedure. These preliminary results seem to confirm the hypothesis cited above on the kinematics of different sized latex particles of different size toward equilibrium position in channel thickness.

### 3.4. SdFFF efficiency

When using standard latex populations of different size distributions, the CV% of each population with their HETP can be correlated as shown in Fig. 6B. Different peak standard

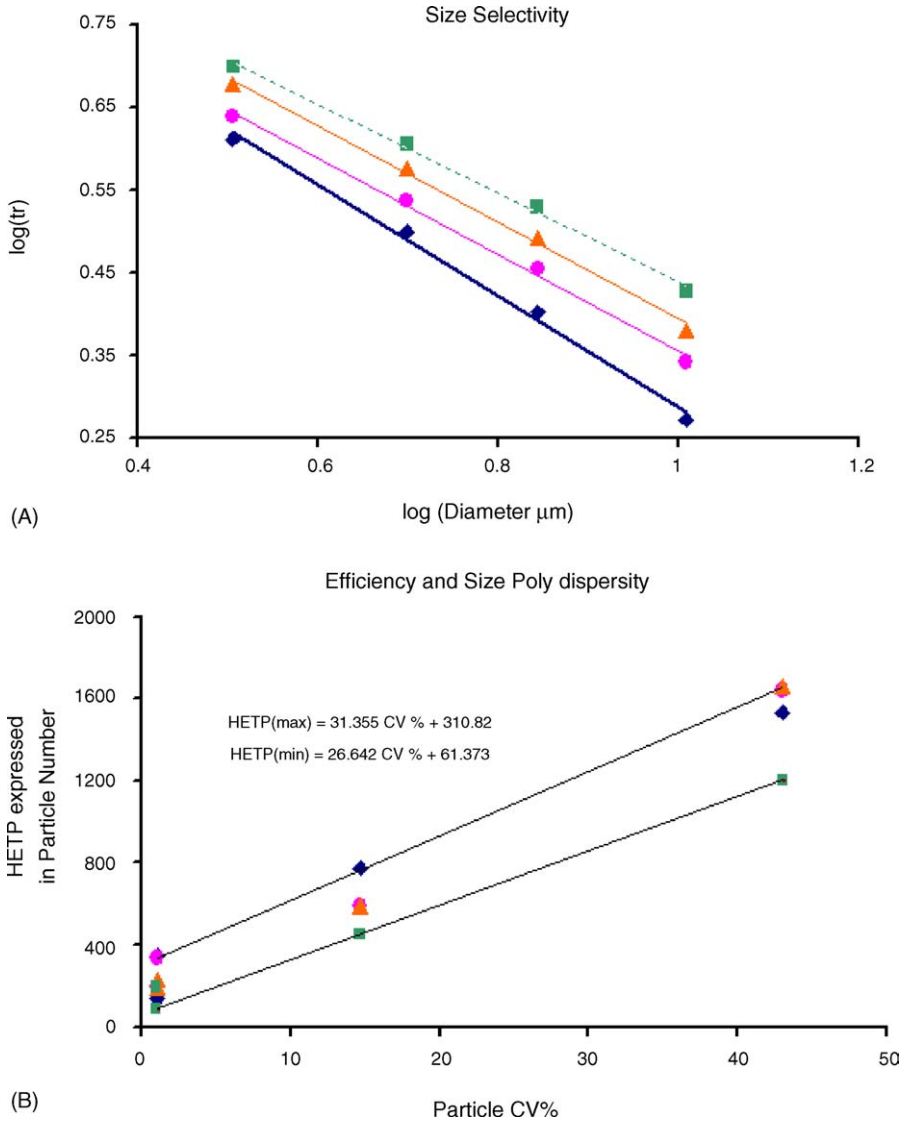


Fig. 6. Size selectivity and HETP in channel II. (A) Size selectivity curves; (B) HETP vs. CV%. A (◊); B (●); C (▲); and D (■) correspond to elution conditions described in Fig. 5.

deviation and retention calculation procedures (moments, mode, and peak height fraction) were calculated for every latex population in the four elution conditions (Fig. 5), providing for each particle a set of HETP values. For every population and every experimental condition, largest and lowest HETP values were selected. Fig. 6B shows the correlation graph of these mini and maxi HETP with particle size distribution, expressed in CV%. HETP is presented in terms of particle number, that is the HETP calculated value in length divided by the particle average diameter. In SdFFF, size polydispersity plays a critical role in terms of HETP contribution [32]. However, the contribution of size polydispersity to HETP, in the Steric Hyperlayer elution mode, remains difficult to assess at present. The correlation curves in Fig. 6B encompass possible HETP values within the experimental domain (field and flow) explored. It experimentally predicts band spreading values. Once average and CV% size are given, using the hypothesis of homogenous and constant density over the size distribution domain; this correlation opens wide opportunities for separations, in particular, in the case particles that are widely dispersed in size. The large HETP obtained for 3 and 10 μm particles suggests that fractions can be collected within the 3 μm (or 10 μm) latex elution peak leading to subpopulations of reduced size distributions. The possible interest of such correlations and HETP a-dimensional description is also demonstrated if Fig. 5 fractograms are reconsidered. Ten micrometer latex beads were eluted first; the observed band spreading was larger than those seen on 5 and 7 μm latex bead peaks. Such possibilities are at the foundation for the use of SdFFF for cell sorting as already published [8].

## 4. Conclusions

Considerable attention must be drawn in terms of instrumentation for successful separations using SdFFF. Channel geometry has to be controlled not only for an accurate void volume. The retention of monodispersed standard particles is also required whose peak profile must appear monomodal, even at a low retention ratio. The design of the inlet tubing connected to the accumulation wall avoids any stop flow injection procedure and accelerates separation development sequences. This design appears effective with 80–100 μm channels. Fig. 3 shows the single sequence, of field dependent separation development for the first time. However, separations may require high retention confining the species close to the accumulation wall and thus, increasing particle/wall interactions leading to, reversible or not, particle trapping. This can be minimized using appropriate flow/field balance as well as specific carrier phase/channel wall combinations. So far trapping minimization procedures were performed with empirical success for cell sorting. However, many questions remain open in that domain. The separation performances of the two laboratory designed systems presented in this report appear close to those previously published [28–30], and justify a posteriori their success in cell sorting [8–32]. The methodology developed in this report has been strongly influenced by one of the first demonstrations of latex bead separation performed by Koch and Giddings with SdFFF [33] 20 years ago. HETP calculations obtained from these data [33] for the series of 3% CV particles are correlated with those of Fig. 6B. These latex separations combined with the pioneering work of Caldwell on the existence of lifting forces in cell sorting [34] were at the origin of the development of cell sorting in SdFFF. If this instrumentation with field programming [35] is combined, considerable versatility is offered. Latex particles of selected and certified size distributions are versatile tools to characterize separation performances in SdFFF when size discrimination is needed.

## Acknowledgements

James R. Kassab wishes to acknowledge the Lebanese national council for scientific research (LNCRS) for a fellowship grant in the year 2003–2004. P. Reschiglian is fully acknowledged for the gift of FL70 surfactant used in this report. That work was made possible by a set of grants involving: DAAD-NaBipa IQN, Aide Régionale à la Recherche en Limousin 2002-S792 and Action Concertée Incitative Technologie pour la Santé (AC-TS-9-2001). Mrs. Jenny Cook-Moreau is fully acknowledged for English language corrections.

## References

[1] J.C. Giddings, Sep. Sci. 1 (1996) 123.
[2] J.C. Giddings, P.S. Williams, Am. Lab. 25 (1993) 88.
[3] J.C. Giddings, S.K. Ratanathanawongs, M.H. Moon, KONA: Powder Particle 9 (1991) 200.
[4] P.J.P. Cardot, C. Elga, M. Guernet, D. Godet, J.P. Andreux, J. Chromatogr. B 654 (1994) 193.
[5] A. Fox, L.E. Schallinger, J.J. Kirkl, K. Microbiol, Methods 3 (1985) 273.
[6] S. Rasouli, E. Assidjo, T. Chianéa, P.J.P. Cardot, J. Chromatogr. B 754 (2001) 11.
[7] S. Battu, A. Roux, S. Delabasee, C. Bosgiraud, P.J.P. Cardot, J. Chromatogr. B 751 (2001) 131.
[8] L. Guglielmi, S. Battu, M. Le Bert, J.L. Faucher, P.J.P. Cardot, Y. Denizot, Anal. Chem. 76 (2004) 1580.
[9] J.C. Giddings, Science 260 (1993) 1456.
[10] H. Cölfen, M. Antonietti, Adv. Polym. Sci. 150 (2000) 67.
[11] M.E. Schimpf, K.D. Caldwell, J.C. Giddings, Field Flow Fractionation Handbook, Wiley-Interscience, New York, 2000.
[12] R. Sanz, I. Puignou, P. Reschiglian, M.T. Galceran, J. Chromatogr. A 919 (2001) 339.
[13] C. Bories, P.J.P. Cardot, V. Abramowski, C. Poüs, A. Merino-Dugay, B. Baron, G. Mougeot, J. Chromatogr. 579 (1992) 143.
[14] A. Bernard, C. Bories, P.M. Loiseau, P.J.P. Cardot, J. Chromatogr. 664 (1995) 444.
[15] E. Assidjo, T. Chianéa, M.F. Dreyfuss, P.J.P. Cardot, J. Chromatogr. B 709 (1998) 197.
[16] J. Chmelík, J. Chromatogr. A 845 (1999) 285.
[17] M. Martin, P.S. Williams, in: F. Dondi, G. Guiochon (Eds.), Theoretical Advancement in Chromatography and Related Separation Techniques, Netherlands, 1992, p. 513.
[18] P.S. Williams, T. Koch, J.C. Giddings, Chem. Eng. Commun. 111 (1992) 121.
[19] P.S. Williams, S. Lee, J.C. Giddings, Chem. Eng. 130 (1994) 143.
[20] K.D. Caldwell, T.T. Nguyen, M.T. Murray, M.N. Myers, J.C. Giddings, Sep. Sci. Technol. 14 (10) (1979) 935.
[21] A. Merino-Dugay, P.J.P. Cardot, M. Guernet, J.P. Andreux, J. Chromatogr. 579 (1992) 73.
[22] E. Elyaman, S. Battu, J. Hugon, P.J.P. Cardot, BBA 1528 (2001) 89.
[23] P.J.P. Cardot, S. Battu, A. Simon, C. Delage, J. Chromatogr. B 768 (2002) 285.
[24] P.J.P. Cardot, P. Trolliard, E. Guernet-Nivaud, Chromatographia 33 (7–8) (1992) 361.
[25] B.N. Barman, J.C. Giddings, Langmuir 8 (1992) 51.
[26] C.J. Van Oss, J. Mol. Recognit. 10 (5) (1997) 203.
[27] M.N. Bellon-Fontaine, J. Rault, C.J. van Oss, Colloids Surf. B: Biointerfaces 7 (1–2) (1996) 47.
[28] Y. Euy Kyung, Kongop Hwahak 11 (8) (2000) 847.
[29] B.N. Barman, J.C. Giddings, J. Calvin, ACS Symp. Ser. 521 (1993) 30.
[30] T. Hoshino, M. Suzuki, K. Ysukawa, M. Takeuchi, J. Chromatogr. 400 (1987) 361.
[31] J.M. Davis, in: M.E. Schimpf, K.D. Calwell, J.C. Giddings (Eds.), Field Flow Fractionation Handbook, Wiley Interscience, New York, USA, 2000, p. 49.
[32] R. Sanz, P. Cardot, S. Battu, M.T. Galceran, Anal. Chem. 74 (17) (2002) 4496.
[33] T. Koch, J.C. Giddings, Anal. Chem. 58 (1986) 994.
[34] K.D. Caldwell, Z.Q. Cheng, P. Hradecky, J.C. Giddings, Cell Biophys. 6 (1984) 233.
[35] F.J.F. Yang, M. Myers, J.C. Giddings, Anal. Chem. 46 (1974) 1924.